journal

J. Am. Ceram. Soc., 88 [4] 875–881 (2005)
DOI: 10.1111/j.1551-2916.2004.00141.x

Properties and Crystallization of Rare-Earth Si–Al–O–N Glasses Containing Mixed Trivalent Modifiers

Michael J. Pomeroy, Elizabeth Nestor, Raghavendra Ramesh,[‡] and Stuart Hampshire[*,†]

Materials and Surface Science Institute, University of Limerick, Limerick, Ireland

Thirteen glasses of the general formula (M1, M2)$_{9.33}$Si$_{14}$Al$_{5.33}$O$_{41.5}$N$_{5.67}$ where M1 = La or Nd and M2 = Y or Er have been prepared with M1/(M1+M2) fractions of 1, 0.75, 0.5, 0.25, and 0. Data for molar volume (MV), glass compactness (*C*), Young's modulus (*E*), microhardness (*H*), glass transition temperatures (T_g), and dilatometric softening temperatures (T_d) have been recorded. In addition, temperatures at which crystallization exotherms arise have also been determined as well as crystalline phases present after the glasses had been heat treated to 1300°C in nitrogen. The results clearly demonstrate that glass properties vary linearly with effective cation field strength (CFS) of the combined modifiers (M1, M2), which is calculated from the atomic fractions of M1 and M2 and their associated CFSs. Glass stability in both the La–Y and La–Er systems reaches a maximum at M1 and M2 fractions of 0.5 because of the relative stability of different oxynitride and disilicate phases with changes in ionic radius. Furthermore, La appears to stabilize the α polymorph of yttrium disilicate because of combined La–Y ionic radius effects.

I. Introduction

A SIGNIFICANT body of work exists in the literature relating to glass-forming regions in metal (M) oxide(s)—silica—silicon nitride systems and also related M–Si–Al–O–N systems, and it is clear that increased nitrogen levels as well as variations in cation ratios result in improved glass properties.[1–14] Some detailed studies[3,5,6,10] have clearly demonstrated that, for a glass with a constant cation ratio, increases in nitrogen content result in increases in hardness, Young's modulus, glass transition temperature, viscosity, and a reduction of thermal expansion coefficient. Pomeroy *et al.*[14] have shown a clear linear correspondence between molar volume (MV), glass compactness, Young's modulus, glass transition temperature, and dilatometric softening temperature and equivalent nitrogen content when the cation ratios Y:Si:Al, Mg:Si:Al, and (Mg,Y):Si:Al are held constant. The explanation for these observations involves increases in the rigidity of glass structure due to trivalent nitrogen species, causing greater cross-linking of the silicate glass network as first suggested by Mulfinger.[15] Some structural studies[16–20] have identified that the glass network contains Si(O$_4$), Si(O$_3$N), and Si(O$_2$N$_2$) tetrahedral structural groups with nitrogen usually present in threefold coordination within the structural network as Si–N bonds, but also can be bonded to one or two silicons. While no clear effect of nitrogen content on the relative fractions of N≡(SiO$_3$)$_3$, –N = (SiO$_3$)$_2$ or >N–(SiO$_3$) has been elucidated from such studies, Pomeroy *et al.*[14] argue that the degree of partitioning of nitrogen to each of these potential species is probably independent of nitrogen content; otherwise, the strong linear property value—nitrogen content correlations they observe would not arise.

Drew *et al.*[3] provided some of the first clear evidence to demonstrate that for glasses in M–Si–Al–O–N systems (M = Mg, Ca, Nd, Y) with the same composition except for changing modifier (M), hardness, viscosity, and glass transition temperature increased in the order Mg<Ca<Nd<Y. Ohashi *et al.*[6] conducted studies on a series of rare-earth–silicon oxynitride glasses with the same M:Si:O:N ratios (M = Y, La, Ce, Nd, Gd, Dy, Er) and observed a reasonably linear increase between the elastic moduli or glass transition temperatures and cation field strength (CFS). A linear decrease in MV is observed with increasing CFS. Similar linear trends have been observed for rare-earth Si–Al–O–N glasses.[9,10] In explaining their results, Ohashi *et al.*[6] and Ramesh *et al.*[9] consider cations with higher CFS values to bond the glass network together more tightly by exerting a greater attraction toward surrounding O and N anions. Because of the linear nature of the trends observed, it was concluded that the basic network structure of these glasses is the same in all cases and that it is merely the CFS that controls glass rigidity and corresponding differences in properties. However, because CFS is related to cation radius, increased glass rigidity may simply be a result of a contraction of the glass network around smaller lanthanide cations.

Few studies have been conducted using mixed-modifier cations (i.e., cations other than Si^{4+} and Al^{3+}), but these studies[21–23] typically investigate the effects of nitrogen substitution for oxygen rather than the effects of mixed cation modifier compositions or ratios. Weldon *et al.*[24] have presented some preliminary results for La–Er-modified Si–Al–O–N glasses, which indicated that changes in MV, hardness, and glass transition temperature were found to be controlled by the cationic field strength of the rare-earth modifier La or Er or an effective CFS for a mixed modifier glass with La:Er = 1:1. The correlation coefficients for changes in the three properties with effective CFS were all greater than 0.985, suggesting that further examination of linear trends between effective CFS and property data would be useful.

In addition to property variations observed for yttrium or different rare-earth-modified glasses, crystallization products can vary widely, too. Thus, Mandal *et al.*[25,26] have reported the effects of cation (M) radius on the oxynitride phases formed during the devitrification of lanthanide (Ln)-modified Si–Al–O–N glasses showing that, for larger radius cations (La, Nd, Sm, etc.), W-phase ($Ln_4Si_9Al_5O_{30}N$) forms, while for smaller radius cations (Y, Er, etc.), B-phase (Ln_2SiAlO_5N) or disilicates ($M_2Si_2O_7$) are more stable. Weldon *et al.*[24] showed that, for the mixed modifier (La:Er = 1:1) glass, devitrification to apatite occurred rather than a biphasic mixture of the La–W-phase and yttrium disilicate, which were the primary devitrification products of the single modifier (La or Er) Si–Al–O–N glasses. Chen *et al.*,[27] in a study of a mixed modifer La–Y–Si–O–N glass, also observed the crystallization of apatite.

With respect to disilicates, Liddell and Thompson[28] have evaluated the effects of cation radius on the stability of various yttrium and lanthanide disilicates and endorsed earlier work that shows that, in general, α-polymorphs are stable for large

P. Becher—contributing editor

Manuscript No. 10452. Received August 7, 2003; approved May 10, 2004.
*Member, American Ceramic Society.
†Author to whom correspondence should be addressed. e-mail: stuart.hampshire@ul.ie
‡Present address: Littelfuse Ireland Limited, Dundalk, Co. Louth, Ireland.

radius cations while β-polymorphs are stable for small radius cations. However, the situation is complex for yttrium disilicates where five polymorphs exist and their relative stabilities are temperature dependent. Thus, Ramesh *et al.*[29] showed that the controlled devitrification of a Y–Si–Al–O–N glass can yield a mixture of α, β, γ, and δ polymorphs depending on heat treatment times and temperatures. Given that yttrium disilicates are the most likely devitrification products of residual intergranular glasses in silicon nitride and low *z*-value sialon materials densified with yttrium oxide, the occurrence of five polymorphs is likely to induce microstructural changes if the polymorph present after crystallization is unstable during service over the time period the ceramic is held at the necessary operating temperature.

The work reported here was designed to develop a clearer understanding of the factors controlling the properties of glasses containing mixed modifiers (La or Nd), (Y or Er) and to examine how the relative stabilities of various likely crystallization products for single-modifier glasses might be affected by the presence of a second modifier cation.

II. Experimental Procedures

(1) Preparation of Glasses

The compositions of the La–Y–Si–Al–O–N, La–Er–Si–Al–O–N and Nd–Y–Si–Al–O–N glasses studied are given in Table I. Glass compositions are expressed in equiv% cations and anions, the calculation of which has been detailed by Drew *et al.*[3] The glasses were prepared by wet mixing the required amounts of La_2O_3, Y_2O_3, Er_2O_3, Nd_2O_3 (Rare Earth Products, Ltd., Suffolk, U.K.) with SiO_2 (Fluka, Buchs, Switzerland), Al_2O_3 (BDH, Poole, U.K.), and Si_3N_4 (Starck grade M11, Goslar, Germany) in isopropanol. Compositions were adjusted to take into account surface silica on the silicon nitride. Following mixing, the powders were dried and each batch was pressed into 50 g pellets at a pressure of 600 MPa using a 20 mm steel die. These pellets were melted in boron nitride-lined graphite crucibles located in a pure alumina work tube within a lanthanum chromite vertical tube furnace. Melting was effected at a temperature of 1700°C for 1 h in a nitrogen environment at 0.1 MPa pressure. Following melting, the glass melt was rapidly withdrawn from the hot zone of the furnace and poured into a preheated graphite mold, where it was annealed for 1 h at 850°C, prior to slow furnace cooling in a muffle furnace. After cooling selected glasses (e.g., singly modified Y–, Nd–, and Er–Sialon glasses and the 14 equiv% La or Nd: 14 equiv%), Er-, or Y-containing glasses were subjected to nitrogen analysis using a Carlo Erba 1106 elemental analyzer (Carlo Erba, Milan, Italy).

(2) Determination of Glass Properties

The amorphous nature of the glass compositions was verified by subjecting them to X-ray diffraction (XRD) using an X'Pert diffractometer PANalytica, Cambridge, U.K.) with Cu*K*α radiation. The chemical homogeneity of the glasses was examined using backscattered electron microscopy (BSEM). Densities of the glasses were determined by the Archimedes method using distilled water as the medium. These density values were used to calculate the MVs of the glasses using the equation:

$$\mathrm{MV} = \frac{\Sigma x_i M_i}{\rho} \tag{1}$$

where x_i and M_i represent the mole fractions and molecular weights of La_2O_3, Y_2O_3, Er_2O_3, Nd_2O_3, Al_2O_3, Si_3N_4, and SiO_2, respectively, and ρ is the measured glass density (g/cm^3). Fractional glass compactness values were calculated using the expression:

$$C = \{\Sigma(x_i V_i.N)\}/\mathrm{MV} \tag{2}$$

where V_i is the ion volume calculated using the data given by Shannon[30] for silicon and aluminum in fourfold coordination and La, Nd, Y, and Er in sixfold coordination. Errors of 0.01 Å in ionic radii data were used in these calculations and those for effective CFS, which are described later.

Microhardness measurements were made on polished samples using a Leco Microhardness Tester (Leco, Stockport, U.K.). A 100 g load was used and 10 microhardness measurements were made on specimens of each glass. Prior to testing, the instrument was calibrated against a standard of known hardness. Elastic and shear moduli were measured using an ultrasonic technique.[31] The velocities of shear waves (V_s) and compressional waves (V_c) were measured using an ultrasonic pulse echo method. Four experiments were conducted for each glass. The elastic (E) and shear (G) moduli were calculated from the following equations:

$$E = \rho V_s^2/(3V_c^2 - 4V_s^2) \tag{3}$$

$$G = \rho V_s^2 \tag{4}$$

Differential thermal analysis (DTA) was carried out using a Stanton Redcroft 1640 series simultaneous DTA instrument

Table I. Compositions of Glasses Studied

La–Y series	e/o La	e/o Y	e/o Si	e/o Al	e/o O	e/o N
28 La 0 Y	28	0	56	16	83	17
21 La 7 Y	21	7	56	16	83	17
14 La 14 Y	14	14	56	16	83	17
7 La 21 Y	7	21	56	16	83	17
0 La 28 Y	0	28	56	16	83	17
La–Er series	**e/o La**	**e/o Er**	**e/o Si**	**e/o Al**	**e/o O**	**e/o N**
28 La 0 Er	28	0	56	16	83	17
21 La 7 Er	21	7	56	16	83	17
14 La 14 Er	14	14	56	16	83	17
7 La 21 Er	7	21	56	16	83	17
0 La 28 Er	0	28	56	16	83	17
Nd–Y series	**e/o Nd**	**e/o Y**	**e/o Si**	**e/o Al**	**e/o O**	**e/o N**
28 Nd 0 Y	28	0	56	16	83	17
21 Nd 7 Y	21	7	56	16	83	17
14 Nd 14 Y	14	14	56	16	83	17
7 Nd 21 Y	7	21	56	16	83	17
0 Nd 28 Y	0	28	56	16	83	17

e/o = equivalent%.

(Polymer Laboratories, Shropshire, U.K.) to determine the glass transition temperatures (T_g) and the various temperatures corresponding to maxima in crystallization exotherms (T_c). Forty milligram powder samples were placed in boron nitride-lined platinum crucibles and subjected to a heating rate of 20°C/min from ambient temperature to 1300°C in a flowing nitrogen environment. The glass transition temperature quoted in the Results section represents the point of inflection of the endotherm corresponding to this secondary transition. Glass softening temperatures (T_d) and coefficients of thermal expansion (α) for each glass were determined using a Netzch (model 402C, Selb, Germany) dilatometer, using polished samples of typical dimensions 10 mm × 4 mm × 3 mm. A heating rate of 5°C/min was used and the corresponding increase in sample length measured using a displacement gauge accurate to 1.25 nm. The coefficients of thermal expansion for each glass are reported as the average value over the temperature range 100°–800°C. During these analyses, the Netzch instrument was calibrated using an α alumina standard.

Following DTA, specimens were subjected to XRD analysis in order to determine the phase assemblages resulting from this continuous heat treatment schedule. In addition to identifying the phases present, the relative X-ray intensities above background levels due to mixed crystalline plus residual amorphous phase or amorphous phase only were calculated and the extents of crystallization were interpolated from these relative intensity data.

Effective CFS (ECFS) was calculated using the expression:

$$\mathrm{ECFS} = \{\mathrm{CFS_{M1}}(C_{M1}/(C_{M1}+C_{M2})\} + \{\mathrm{CFS_{M2}} \times (C_{M2}/(C_{M1}+C_{M2})\} \quad (5)$$

where $\mathrm{CFS_{M1}}$ and $\mathrm{CFS_{M2}}$ are the CFSs of the M1 and M2 cations, and $\mathrm{C_{M1}}$ and $\mathrm{C_{M2}}$ are their respective concentrations in atomic percent.

III. Results

(1) Glass Formation

XRD analyses of each of the as-fired glasses confirmed their amorphous nature. The visual appearance of the glass bars suggested that they were homogeneous and this was confirmed by BSEM. La–Y glasses varied in color from light lime green to black as La was replaced by Y. Color variations for the La–Er glasses were from light green to a wine color as La was replaced by Er. For the Nd–Y glasses, color variations from navy blue to black occurred as Nd was replaced by Y. Nitrogen analysis results for selected glasses showed that N losses were minimal, with fired compositions having N contents of within 1 equiv% N of the starting composition. This is consistent with the negligible weight losses (<0.3% of the total weight) during firing recorded for these glasses. Glasses not subjected to nitrogen analysis also showed negligible weight losses during melting, and so similar compositional errors for N losses were assumed.

(2) Physical and Thermal Properties of Glasses

Variations in glass density caused by replacing lanthanum with either yttrium or erbium are given in Table II. As might be expected on the basis of the relative atomic weights of La, Nd, Y, and Er, approximately linear decreases in density are observed as lanthanum or neodymium is replaced by yttrium. A linear increase in density is observed as lanthanum is replaced by erbium. It is to be noted that the changes in density are not solely due to the replacement of one cation by a lighter or heavier cation. In the case of the La–Y sialon glasses, decreases in the density of some 18% would be expected as the formula weight decreases when all lanthanum is replaced by yttrium. The actual decrease in density recorded is some 12%. For the total replacement of lanthanum by erbium, expected and measured increases in density are 10% and 17%, respectively. The discrepancy between measured density and expected densities are explicable if changes in MV are examined. Table II relates these data and indicates that, as the effective CFS increases, the MV decreases, thus explaining the discrepancies referred to above.

Figure 1 shows that there is effectively a linear decrease in MV as the effective CFS increases, and that this is applicable to each of the La–Y, La—Er, and Nd–Y glass series. In addition, the least squares fit for each of the plots shown in Fig. 1 has very similar gradients; indeed, two of the correlations overlap. Given these correlations and, as shown later, similar linear trends between other properties and the effective CFS of the mixed modifiers, MV data for each of the 13 different glasses were analyzed for an overall trend. Figure 2 shows the linear trend for all of the data together with the standard error limits derived from differences between calculated and observed values for all data points (± 0.09 cm^3 mol^{-1}). It is seen from Fig. 2 that virtually the entire data points fit linear plots within the error limits. Accordingly, given experimental errors and possible variations in glass preparation (powder weighing, cooling rate, annealing rate, density measurement), it would appear that there is a clear relationship between MV and the effective CFS of the mixed

Table II. Properties of Glasses

		Effective CFS of modifier (Å^{-2})	Density (g cm^{-3})	Molar volume (cm^3 mol^{-1})	Fractional glass compactness	Young's modulus (GPa)	Microhardness (GPa)	T_g onset (°C)	T_g midpoint (°C)	T_{ds} (°C)	CTE (10^{-6}. K^{-1})
La	**Y**										
28	0	2.66±0.05	4.33	7.84	0.4217	130	8.69	905	916	924	7.2
21	7	2.94±0.06	4.21	7.70	0.4246	134	8.90	919	934	932	6.8
14	14	3.21±0.07	4.05	7.62	0.4239	143	9.63	935	945	932	6.8
7	21	3.49±0.07	3.91	7.50	0.4256	149	9.70	948	957	959	6.3
0	28	3.76±0.08	3.78	7.35	0.4291	156	10.22	953	969	978	6.2
La	**Er**										
28	0	2.66±0.05	4.33	7.84	0.4217	130	8.69	905	916	924	7.2
21	7	2.97±0.06	4.47	7.79	0.4193	129	9.38	913	929	938	7.0
14	14	3.27±0.07	4.71	7.58	0.4258	138	9.82	920	936	955	6.5
7	21	3.57±0.08	4.95	7.39	0.4314	145	9.95	948	958	951	6.4
0	28	3.87±0.09	5.05	7.41	0.4244	147	10.50	960	973	967	6.3
Nd	**Y**										
28	0	3.03±0.06	4.51	7.67	0.4223	136	9.50	916	931	916	7.0
21	7	3.21±0.07	4.31	7.63	0.4217	135	9.53	917	933	928	6.7
14	14	3.40±0.07	4.11	7.59	0.4213	137	9.53	940	950	956	6.5
7	21	3.58±0.08	3.92	7.52	0.4222	145	10.13	943	953	957	6.4
0	28	3.76±0.08	3.78	7.35	0.4291	156	10.22	953	969	978	6.2

CFS, cation field strength; T_g, glass transition temperature; T_{ds}, dilatometric softening temperature; CTE, coefficient of thermal expansion.

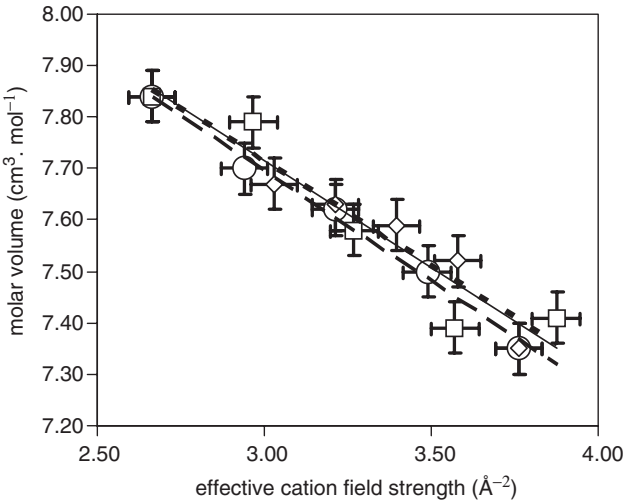

Fig. 1. Effect of cation field strength on molar volumes of La–Y (○), La–Er (△), and Nd–Y (□) glasses (straight lines are correlations for individual glass groups).

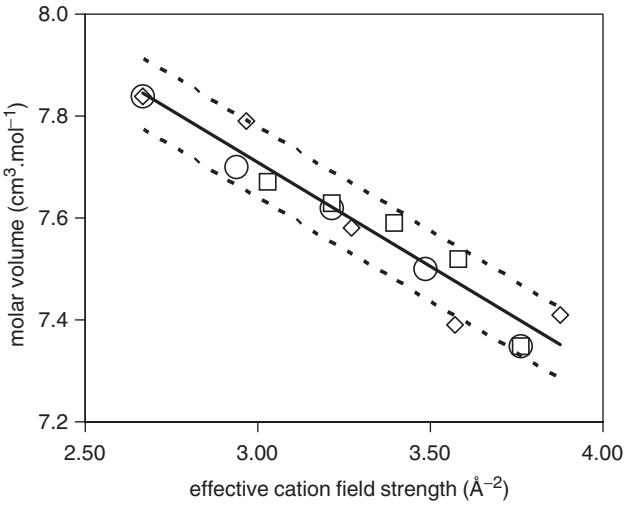

Fig. 2. Effect of cation field strength on molar volumes for all glasses: La–Y (○), La–Er (△), and Nd–Y (□) (solid line is the regression line for all data points, dashed lines are $\pm 1.5 \times$ standard error value).

modifier. The intercept and linear slope coefficients for MV—effective field strength correlation are given in Table III.

Modulus data are given in Table II. Again, plotting these data against the effective CFS of the modifier showed a linear trend and the corresponding intercept, slope, and error limit values are given in Table III. Young's modulus also shows a linear increase with increasing effective CFS (Fig. 3) as does hardness, glass transition temperature (Fig. 4), and dilatometric softening temperature. Intercept, slope, and error limit values for these three properties are also given in Table III. Thermal expansion coefficients were observed to decrease linearly with increasing effective CFS as shown in Fig. 5. The associated data analysis results are also given in Table III. While similar sources of error arise for modulus, microhardness, glass transition temperature, dilatometric softening temperature, and coefficient of thermal expansion as for MV, errors for modulus, microhardness, and coefficient of thermal expansion (Figs. 3–5) are compounded by specimen preparation.

(3) Crystallization of La–Y and La–Er Glasses

Table IV shows the variation in the temperature of the first, and major, crystallization event for the La–Y and La–Er glasses. The data show that, as lanthanum is substituted by 7 equiv% of either yttrium or erbium, little change is observed in this crystallization temperature. With 14 equiv% yttrium or erbium substitution, the first crystallization temperature increases further and, in addition, the crystallization temperature for the La–Er glass is higher than for the La–Y counterpart, suggesting that crystallization is more difficult in the system containing erbium. At 21 equiv% substitution, a further increase in crystallization temperature is noted for the La–Y glass, but a slight decrease occurs for the La–Er glass. A decrease in crystallization temperature for the glass containing 28 equiv% yttrium indicates the crystallization of a different silicate than arises for the glass containing 21 equiv% yttrium as is related below. At 28 equiv% Er substitution, a further increase in crystallization temperature is noted.

Table V shows the major phase(s) present in the glasses following their heat treatment to 1300°C. For the La–Si–Al–O–N glasses, the phases formed are lanthanum disilicate and lanthanum W-phase ($La_4Si_9Al_5O_{30}N$). For both yttrium and erbium substitutions of 7 equiv%, the phase assemblage is the same, although the glass seems to be more stable as crystallinity levels are lower (see Fig. 6). The phase formed at the 14 equiv% yttrium or erbium substitution levels, while difficult to identify, is thought to be La–M2 (M2 = Y or Er) apatite, which would be consistent with analyses of a similar La–Er glass containing 20 equiv% nitrogen[32] and observations by Chen *et al.*[27] for La–Y–Si–Al–O–N glasses. As the substitution levels are increased beyond 14 equiv% Y or Er, silicates are observed and, in the case of the Er-containing glasses, erbium aluminate. What is interesting is that there is only one polymorph of yttrium disilicate (α) present when the glass contains 7 equiv% La, while two polymorphs (α and β) are observed when no lanthanum is present. This strongly suggests that lanthanum stabilizes the α-yttrium disilicate polymorph.

Figure 6 shows the variation in levels of crystallinity after the DTA runs to 1300°C with increasing yttrium or erbium substitution for lanthanum. It is seen that as the replacement of La by Y or Er increases from 0 to 14 equiv%, the level of crystallinity decreases to a minimum and then increases again as 21 and 28 equiv% La is replaced by either Y or Er. Given that the accuracy of the determination method is of the order of $\pm 5\%$, it appears that there is little difference in the relative levels of crystallinity between the La–Y and La–Er systems. From the

Table III. Least-Squares Intercepts and Slopes for Linear Correlations Between Properties and Effective Cation Field Strength for All Glasses

Property	Least-squares intercept	Least-squares slope	Standard error
Molar volume	8.95 cm^3/mol	$-0.4\ cm^3 \cdot mol^{-1} \cdot Å^{-2}$	$\pm 0.07\ cm^3 \cdot mol^{-1}$
Young's modulus	73.1 GPa	20.5 Gpa/$Å^2$	± 4 GPa
Microhardness	4.9 GPa	1.4 GPa/$Å^2$	± 0.3 GPa
Glass transition temperature (onset)	778°C	46.8°C/$Å^2$	± 6°C
Glass transition temperature (midpoint)	790°C	46.9°C/$Å^2$	± 4°C
Dilatometric softening temperature	795°C	45.9°C/$Å^2$	± 10°C
Coefficient of thermal expansion	$9.4 \times 10^{-6}\ K^{-1}$	$-0.8 \times 10^{-6}\ K^{-1} \cdot Å^{-2}$	$\pm 0.1 \times 10^{-6}\ K^{-1}$

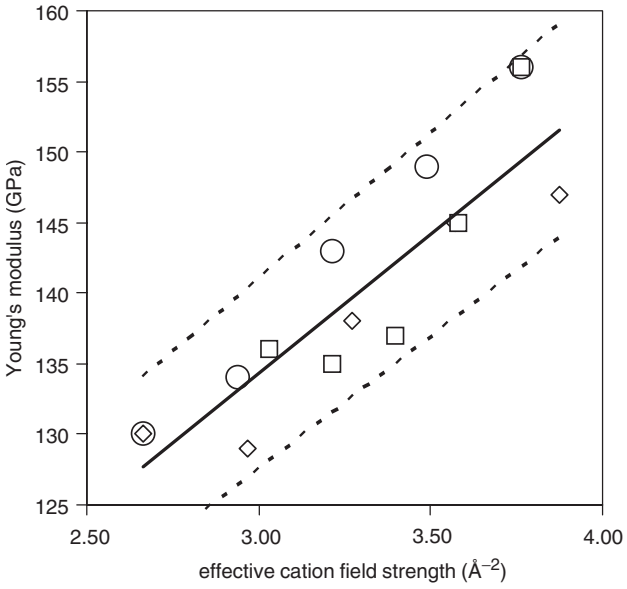

Fig. 3. Effect of cation field strength on Young's modulus for all glasses: La–Y (○), La–Er (△), and Nd–Y (□) (solid line is the regression line for all data points, dashed lines are ±1.5 × standard error value).

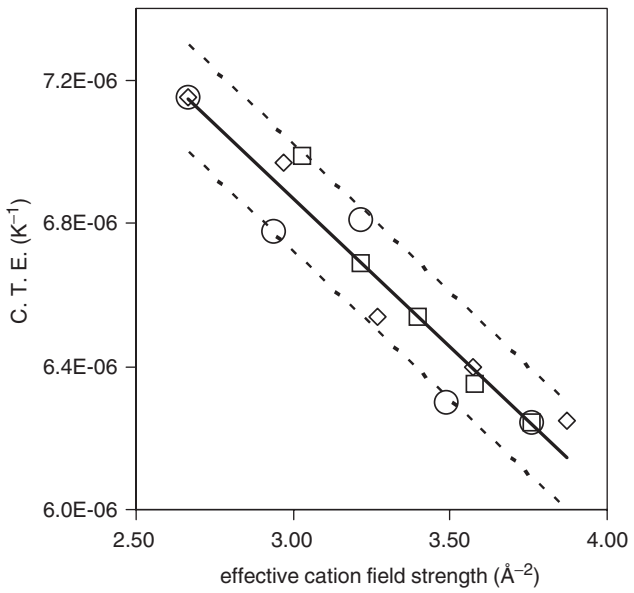

Fig. 5. Effect of cation field strength on coefficient of thermal expansion for all glasses: La–Y (○), La–Er (△), and Nd–Y (□) (solid line is the regression line for all data points; dashed lines are ±1.5 × standard error value).

data presented, however, it can be inferred that as the La:Y or La:Er ratio approaches 1:1, the mixed-modifier glass becomes more stable with respect to the crystalline phase formed by heat treatment, in this case apatite.

IV. Discussion

(1) Glass Properties

From the above analysis of glass property results, it is seen that MV and thermal expansion coefficient values decrease with increasing effective CFS while fractional glass compactness, modulus, microhardness, glass transition temperature, and dilatometric softening temperature values increase with increasing effective CFS. As the correlation between each property and effective CFS is linear, then all other factors are expected to be equal. Thus, the overall glass network structure comprising cross-linked $(Si,Al)(O,N)_4$ tetrahedra, with the necessary number of cross-links being replaced by non-bridging oxygens, must be the same irrespective of the modifier cations in the system. Furthermore, it appears that the number of aluminum ions in five- and sixfold coordination must also be very similar. Given that the glass structure is virtually the same for each glass, it must be the bonding strength with which the modifier cations associate non-bridging oxygens in adjacent parts of the glass structure that gives rise to the property trends observed. A simple measure of this strength of association is, of course, the effective CFS, as has also been shown for similar glass systems containing single modifiers.[6,9] Furthermore, assessment of data for glass transition temperatures and dilatometric softening temperatures published by Shelby and Kholi[33] for oxide glasses containing Nd–Y or Nd–Er mixed modifiers, using the effective CFS approach, again gives rise to good straight-line correlations, albeit for different cation ratios (25 equiv% (M1, M2):25 equiv% Al:50 equiv% Si). It is therefore concluded that, all other factors being equal, the effective CFS controls glass properties in rare-earth Si–Al–O–N glasses containing mixed-modifier cations. It is to be noted, however, that this conclusion is only valid for mixed modifier cations with the same valency. In mixed modifier systems where cation valencies are not equal, such as for Mg–Y–Si–Al–O–N glasses,[14] other correlations are required to explain property variations with substitutions of a divalent by a trivalent cation.

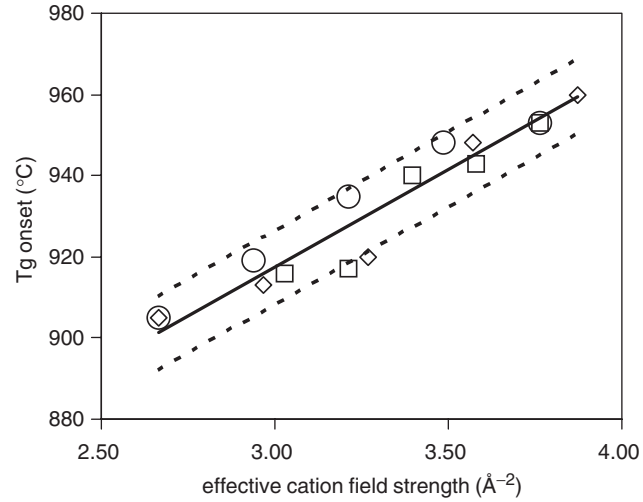

Fig. 4. Effect of cation field strength on glass transition temperature for all glasses: La–Y (○), La–Er (△), and Nd–Y (□) (solid line is the regression line for all data points, dashed lines are ±1.5 × standard error value).

(2) Crystallization of Glasses

From the results presented, it is seen that the crystallization of the more lanthanum-rich glasses occurs at lower temperatures

Table IV. Crystallization Temperatures of Glasses

					T_g midpoint (°C) (error ±5°C)	T_c1 (°C)	T_c2 (°C)	T_c3 (°C)
La–Y series								
28	La	0	Y		916	1104	1169	1247
21	La	7	Y		934	1105	1169	1206
14	La	14	Y		945	1118	—	—
7	La	21	Y		957	1134	—	1211
0	La	28	Y		969	1063	1189	1232
La–Er series								
28	La	0	Er		916	1104	1169	1247
21	La	7	Er		929	1111	—	1220
14	La	14	Er		936	1149	—	—
7	La	21	Er		958	1130	1188	1211
0	La	28	Er		973	1151	1212	1240

Table V. Crystallisation Products after DTA Run to Temperature of 1300°C

La–Y–Si–Al–O–N glasses		
La	Y	
28	0	$La_2Si_2O_7$, La–W-phase ($La_4Si_9Al_5(O_{30}N_1)$)
21	7	$La_2Si_2O_7$, La–W-phase ($La_4Si_9Al_5(O_{30}N_1)$)
14	14	Apatite
7	21	α-$Y_2Si_2O_7$
0	28	α-$Y_2Si_2O_7$, β-$Y_2Si_2O_7$
La–Er–Si–Al–O–N glasses		
La	Er	
28	0	$La_2Si_2O_7$, La–W-phase ($La_4Si_9Al_5(O_{30}N_1)$)
21	7	$La_2Si_2O_7$, La–W-phase ($La_4Si_9Al_5(O_{30}N_1)$)
14	14	Apatite
7	21	$Er_2Si_2O_7$, $Er_4Al_2O_9$
0	28	$Er_2Si_2O_7$, $Er_4Al_2O_9$

DTA, differential thermal analysis.

than for those containing equal amounts of La- and Y- or La- and Er- or the Y- or Er-rich glasses. One reason for this is that, as lanthanum has a lower CFS than the other two cations, the glass structure can be less rigid and so can be more readily arranged into the structural components associated with La–W phase and lanthanum disilicate. Such a rationalization would also explain the increasing crystallization temperatures for the La–Er glasses containing more than 7 equiv% erbium and for the La–Y analogues (excepting the Y–Si–Al–O–N glass). A second reason for the observed trends in primary crystallization temperature is that, as lanthanum is substituted by yttrium or erbium, the relative stabilities of the crystalline phases formed compared with the glasses decrease, with the result that the thermal energy required for crystallization also increases. If this were the case, however, the levels of crystallinity after the same heat treatment would be expected to show a decreasing trend with increasing Y and Er levels, and this is clearly not so. Accordingly, it can be concluded that, for all glasses except the Y–Si–Al–O–N glass, crystallization temperatures are determined by the rigidity of the glass structure, and the higher the rigidity of the glass structure, the higher the thermal energy requirement for its crystallization. Glasses with the composition of the Y–Si–Al–O–N investigated here typically devitrify to the y-polymorph of yttrium disilicate initially,[29] and this forms at much lower temperatures than the α or β disilicates formed by La and Er.

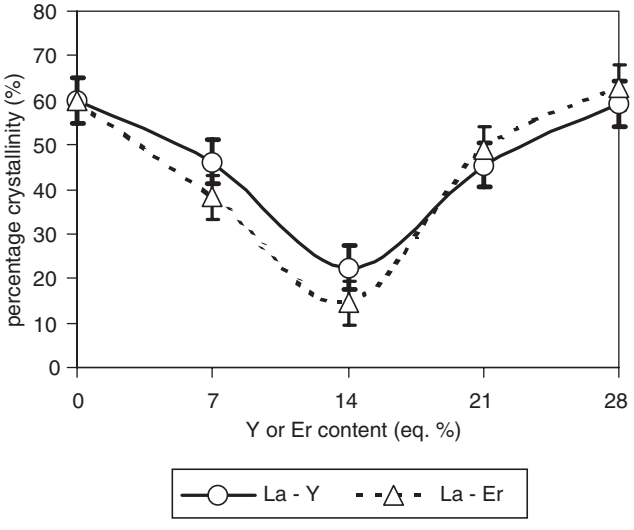

Fig. 6. Effect of M1–M2 cation composition of volume fraction crystallization after differential thermal analysis run to temperature of 1300°C.

The phases formed on heat treatment of the single-modifier (La and Y) Si–Al–O–N glasses are consistent with what might be expected from previous work. Thus, lanthanum W-phase is observed for the La–Si–Al–O–N glass, as previously reported,[25,26] and a mixed $\alpha+\beta$ yttrium disilicate phase assemblage is observed for the Y–Si–Al–O–N glass as previously indicated by Ramesh *et al.*[29] The devitrification of the Er–Si–Al–O–N glass to erbium disilicate would also be expected, given the rare-earth cation radius criterion given by Weldon *et al.*[24] and Mandal *et al.*[25] The occurrence of the aluminate is also consistent with the devitrification of rare-earth Si–Al–O–N glasses containing smaller cations or yttrium,[29] although longer devitrification times are typically required for the aluminate to form.

For the mixed-modifier glasses, the substitution of 7 equiv% La by Y or Er yields the same phase assemblage as the La–Si–Al–O–N glass, although extents of crystallinity are less. These two observations probably indicate that only lanthanum enters the crystalline phases, which might be expected on the basis of previous evidence.[24,25,27] Thus, Er cannot enter the La–W phase lattice to any great extent because its ionic radius is too small, neither can it substitute significantly for La in lanthanum disilicate, which is predominantly the β modification rather than the α-polymorph associated with erbium disilicate. Because of this, Er is most likely to form more stable glasses that would account for the decreased levels of crystallinity observed. For the 14 equiv% substitution level, the formation of apatite is consistent with the previous findings of Weldon *et al.*[24] and Chen *et al.*[27] It is thought that the defect structure of apatite, which typically contains cation vacancies, can facilitate accommodation of both La and Y or La and Er cations. If this is the case, then the formation of such a mixed-modifier-containing apatite would be expected to involve the partitioning of the La and M2 cations. This explanation would be consistent with the low levels of crystallinity observed, since long crystallization times would be required for the necessary partitioning to occur, particularly as first-formed apatite may redissolve in order to reprecipitate with a more stable La:M2 cation ratio.

For the 21 equiv% Er substitution level, the (La, Er)–Si–Al–O–N glass shows exactly the same crystallization behavior as the Er–Si–Al–O–N glass, clearly indicating that the 7 equiv% La in the system has no effect on crystallization products and probably resides in the glass. In contrast, the La–Y-containing glass shows different behavior compared with the Y–Si–Al–O–N glass, in that only the α-polymorph of $Y_2Si_2O_7$ is formed. The effective modifier (La, Y) cation radius for the 7 equiv% La–21 equiv% Y glass (calculated using the expression $r_{c\ eff} = \{r_{c\ La(III)}.(C_{La}/(C_{La}+C_Y)\} + \{r_{c\ Y(III)}.(C_Y/(C_{La}+C_Y)\}$) is 93.5 pm. Superposition of this effective cationic radius on the phase stability regions for disilicates given by Mandal *et al.*[25] and Liddell and Thompson[28] indicates that the α-polymorph should be stable over the temperature range that the glass experienced during its heat treatment in the DTA apparatus. Accordingly, it is very significant that the occurrence of the α-polymorph alone, when the 7 equiv% La–21equiv% Y glass is devitrified, is due to a stabilizing effect of the lanthanum cation. This is a very important indication that is worthy of further study as it may be possible, with appropriate heat treatments, to stabilize the crystalline grain-boundary phases in silicon nitride-based materials densified with yttria before use as high-temperature components.

V. Conclusions

From the work carried out on various mixed modifier M1–M2–Si–Al–O–N glasses (M1 = La or Nd), (M2 = Y or Er), the following conclusions can be drawn:

(1) MV, glass fractional compactness, Young's modulus, microhardness, glass transition temperature (onset and mid-

point), dilatometric softening temperature, and coefficient of thermal expansion are all linearly related to the effective CFS of the mixed modifiers. This strongly indicates that the overall (Si, Al) (O, N) glass network has a similar structure for each of the systems studied and that it is the strength of attraction between the modifier cations and the network, particularly non-bridging anions, which controls glass properties.

(2) For all La–Y and La–Er glasses except the Y–Si–Al–O–N glass, crystallization temperatures are determined by the rigidity of the glass structure and, as this increases, the thermal energy required for crystallization increases. The crystallization temperature for the Y–Si–Al–O–N glass is determined by the fact that the y-polymorph of yttrium disilicate is more stable at lower temperatures than the α or β disilicates formed in the other glasses.

(3) Small substitutions (7 equiv%) of the M1 or M2 cations result in little change to the phase assemblages of the singly modified glasses, excepting that greater levels of residual glass remain as the substituting cation has little solubility in the crystalline phases formed during devitrification. An anomaly arises for the 7 equiv% La—21 equiv% Y-modified glass where the La stabilizes the α-polymorph of yttrium disilicate by La substitution, which modifies the average cation radius.

4) Equi-molar substitution levels (14 equiv% M1, 14 equiv% M2) preclude the formation of disilicates, and apatite is the stable phase formed, although not in significant quantities, such that much more residual glass remains because of slow La, and Y or Er partitioning effects between the glass and the crystallizing apatite.

References

[1]R. E. Loehman, "Preparation and Properties of Yttrium–Silicon–Aluminium Oxynitride Glasses," *J. Am. Ceram. Soc.*, **62**, 491–4 (1979).

[2]R. R. Wusirika and C. K. Chyung, "Oxynitride Glasses and Glass-Ceramics," *J. Non-Cryst. Solids*, **38–39**, 39–44 (1980).

[3]R. A. L. Drew, S. Hampshire, and K. H. Jack, "Nitrogen Glasses" in *Special Ceramics*, **Vol. 7**, Edited by D. E. Taylor and P. Popper. *Proc. Br. Ceram. Soc.*, **31**, 119–32 (1981).

[4]S. Sakka, K. Kamiya, and T. Yoko, "Preparation and Properties of Ca–Al–Si–O–N Oxynitride Glasses," *J. Non-Cryst. Solids*, **56**, 147–55 (1983).

[5]S. Hampshire, E. Nestor, R. Flynn, J. –L. Besson, T. Rouxel, H. Lemercier, P. Goursat, M. Sebai, D. P. Thompson, and K. Liddell, "Yttrium Oxynitride Glasses: Properties and Potential for Crystallisation to Glass-Ceramics," *J. Eur. Ceram. Soc.*, **14**, 261–73 (1994).

[6]M. Ohashi, K. Nakamura, K. Hirao, S. Kanzaki, and S. Hampshire, "Formation and Properties of Ln–Si–O–N Glasses (Ln = Lanthanides or Y)," *J. Am. Ceram. Soc.*, **78** [1] 71–6 (1995).

[7]E. Zhang, K. Liddel, and D. P. Thompson, "Glass Forming Regions and Thermal Expansion of Some Ln–Si–Al–O–N Glasses (Ln = La, Nd)," *Br. Ceram. Trans. J.*, **95** [4] 170–2 (1996).

[8]E. Y. Sun, P. F. Becher, S. L. Hwang, S. B. Waters, G. M. Pharr, and T. Y. Tsui, "Properties of Silicon–Aluminum–Yttrium Oxynitride Glasses," *J. Non-Cryst. Solids*, **208**, 162–9 (1996).

[9]R. Ramesh, E. Nestor, M. J. Pomeroy, and S. Hampshire, "Formation of Ln–Si–Al–O–N Glasses and Their Properties," *J. Euro. Ceram. Soc.*, **17**, 1933–9 (1997).

[10]P. F. Becher, S. B. Waters, C. G. Westmoreland, and L. Riester, "Influence of Composition on the Properties of Si–R–E–Al Oxynitride Glasses: RE = La, Nd, Gd, Y or Lu," *J. Am. Ceram. Soc.*, **85** [4] 897–902 (2002).

[11]G. Leng-Ward and M. H. Lewis, "Oxynitride Glasses and Their Glass-Ceramic Derivatives;" in *Glasses and Glass-Ceramics*, Edited by M. H. Lewis. Chapman & Hall, London, 1990.

[12]D. P. Thompson, "Oxynitride Glasses;" in *High Performance Glasses*, Edited by M. Cable and J. M. Parker. Blackie and Sons, Glasgow, 1992 (Ch. 5).

[13]S. Hampshire, "Oxynitride Glasses, Their Properties and Crystallisation—A Review," *J. Non-Cryst. Solids*, **316**, 64–73 (2003).

[14]M. J. Pomeroy, C. Mulcahy, and S. Hampshire, "Independent Effects of Nitrogen Substitution for Oxygen and Magnesium Substitution by Yttrium on the Properties of Mg–Y–Si–Al–O–N Glasses," *J. Am. Ceram. Soc.*, **86** [3] 458–64 (2003).

[15]H. O. Mulfinger, "Physical and Chemical Solubility of Nitrogen in Glass Melts," *J. Am. Ceram. Soc.*, **49**, 462–7 (1966).

[16]R. K. Brow and C. G. Pantano, "Nitrogen Coordination in Oxynitride Glasses," *J. Am. Ceram. Soc.*, **67**, C72–4 (1984).

[17]W. Hater, W. M. Warmuth, and G. H. Frischat, "^{29}Si MAS NMR Studies of Alkali Silicate Oxynitride Glasses," *Glastechn. Ber.*, **62**, 328–35 (1989).

[18]T. Rouxel, J.-L. Besson, E. Rzepka, and P. Goursat, "Raman Spectra of Si-YAlON Glasses and Ceramics," *J. Non-Cryst. Sol.*, **122**, 298–304 (1990).

[19]J. S. Jin, T. Yoko, F. Miyaji, S. Sakka, T. Fukunaga, and M. Misawa, "Neutron-Diffraction and Solid-State MAS-NMR Studies of the Structure of Y–Al–Si–O–N Oxynitride Glasses," *Philosophical Magazine B—Physics of Condensed Matter Statistical Mechanics Electronic Optical and Magnetic Properties*, **70** [2] 191–203 (1994).

[20]S. Sakka, "Structure, Properties and Application of Oxynitride Glasses," *J. Non-Cryst. Solids*, **181** [3] 215–24 (1995).

[21]J. Chen, J. L. Huang, H. Guo, and H. Le, "Preparation and Properties of La–Y–Si–O–N Oxynitride Glasses," *Trans. Mater. Res. Soc. Jpn*, **16A**, 31–4 (1994).

[22]L. Avignon-Poquillon, B. Viot, P. Verdier, and Y. Laurent, "Verres d'Aluminosilicates Oxygenes et Oxyazotes: Etude des Systemes La–Si–Al–O–N et Mg–La–Si–Al–O–N," *Silicates Industrielles*, **9–10**, 131–40 (1992).

[23]J. Rocherulle, M. Matecki, and Y. Delugeard, "Heat Capacity Measurements of Mg–Y–Si–Al–O–N Glasses," *J. Non-Cryst. Solids*, **238** [1–2] 51–6 (1998).

[24]L. Weldon, M. J. Pomeroy, and S. Hampshire, "Glasses in the Rare-Earth Sialon Systems," *Key Eng. Mater.*, **118–119**, 241–8 (1996).

[25]H. Mandal, D. P. Thompson, and T. Ekstrom, "Heat Treatment of Ln–Si–Al–O–N Glasses," *Key Eng. Mater.*, **72–74**, 187–203 (1992).

[26]H. Mandal, D. P. Thompson, and T. Ekström, "Heat-Treatment of Sialon Ceramics Densified with Higher Atomic Number Rare Earth and Mixed Yttrium/Rare Earth Oxides;" in *Special Ceramics*, **Vol. 9**, Edited by R. Stevens. *Proc. Br. Ceram. Soc.*, **49**, 149–62 (1992).

[27]J. Chen, P. Wei, and Y. Huang, "Formation and Properties of La–Y–Si–O–N Oxynitride Glasses," *J. Mater. Sci. Lett.*, **16** [18] 1486–8 (1997).

[28]K. Liddell and D. P. Thompson, "X-ray Diffraction Data for Yttrium Silicates," *Br. Ceram. Trans. J.*, **85**, 17–22 (1986).

[29]R. Ramesh, E. Nestor, M. J. Pomeroy, and S. Hampshire, "Classical and Differential Thermal Analysis Studies of the Glass-Ceramic Transformation in a Y–Si–Al–O–N Glass," *J. Am. Ceram. Soc.*, **81** [5] 1285–97 (1998).

[30]R. D. Shannon, "Effective Ionic Radii in Oxides and Fluorides," *Acta Crystallogr.*, **B25**, 751–6 (1969).

[31]H. Lemercier, M. Sebai, T. Rouxel, P. Goursat, S. Hampshire, and J. L. Besson, "Yttrium Si–Al–O–N Glasses: Ultrasonic Study of Crystallisation," *J. Eur. Ceram. Soc.*, **17**, 1949–53 (1997).

[32]K. Liddell and D. P. Thompson Private Communication, 1995.

[33]J. E. Shelby and J. T. Kohli, "Rare-Earth Aluminosilicate Glasses," *J. Am. Ceram. Soc.*, **73** [1] 39–42 (1990). □